6488–6495 *Nucleic Acids Research, 2006, Vol. 34, No. 22* *Published online 27 November 2006*
doi:10.1093/nar/gkl867

Use of thermolytic protective groups to prevent G-tetrad formation in CpG ODN type D: structural studies and immunomodulatory activity in primates

Montserrat Puig, Andrzej Grajkowski[1], Malgorzata Boczkowska[2], Cristina Ausín[1], Serge L. Beaucage[1] and Daniela Verthelyi*

Laboratory of Immunology and [1]Laboratory of Chemistry, Division of Therapeutic Proteins, Center for Drug Evaluation and Research, Food and Drug Administration, 8800 Rockville Pike, Bethesda, MD 20892, USA and [2]Department of Physiology, School of Medicine, University of Pennsylvania, 3700 Hamilton Walk, Philadelphia, PA 19104-6085, USA

Received August 23, 2006; Revised September 25, 2006; Accepted October 4, 2006

ABSTRACT

CpG oligodeoxynucleotides (ODN) show promise as immunoprotective agents and vaccine adjuvants. CpG ODN type D were shown to improve clinical outcome in rhesus macaques challenged with *Leishmania major*. These ODN have a self-complementary core sequence and a 3′ end poly(G) track that favors G-tetrad formation leading to multimerization. Although multimerization appears necessary for localization to early endosomes and signaling via Toll-like receptor 9 (TLR-9), it can result in product polymorphisms, aggregation and precipitation, thereby hampering their clinical applications. This study shows that functionalizing the poly(G) track of D ODN with thermolytic 2-(*N*-formyl-*N*-methyl)aminoethyl (*fma*) phosphate/thiophosphate protecting groups (pro-D ODN) reduces G-tetrad formation in solution, while allowing tetrad formation inside the cell where the potassium concentration is higher. Temperature-dependent cleavage of the *fma* groups over time further promoted formation of stable G-tetrads. Peripheral blood cells internalized pro-D ODN efficiently, inducing high levels of IFNα, IL-6, IFNγ and IP-10 and triggering dendritic cell maturation. Administration of pro-D35 to macaques challenged with *L.major* significantly increased the number of antigen-specific IFNγ-secreting PBMC and reduced the severity of the skin lesions demonstrating immunoprotective activity of pro-D ODN *in vivo*. This technology fosters the development of more efficient immunotherapeutic oligonucleotide formulations for the treatment of allergies, cancer and infectious diseases.

INTRODUCTION

Bacterial and synthetic oligodeoxynucleotides (ODN) containing unmethylated CpG dinucleotides in specific sequence contexts (CpG ODN) trigger the vertebrate immune system through the activation of Toll-like receptor 9 [TLR-9 (1,2)]. The resulting innate immune response limits the early spread of infectious organisms, while promoting the development of adaptive immunity. CpG ODN show promise as vaccine adjuvants and in the treatment of asthma, allergy, infection and cancer (1,2).

Optimal sequences for the activation of TLR-9 vary among species (3). Human and non-human primate TLR-9 respond to three types of synthetic CpG ODN: Type D (and A), type K [also referred to as B (1)] and type C, which have distinct structures and immunostimulatory activities (1,4). Oligodeoxyribonucleotides type D and A induce human pDC to secrete high levels of IFNα, which in turn induces monocytes to mature into functionally active DC, and γδT cells and natural killer cells to secrete IFNγ (5–7). In contrast to K or C-type CpG ODN, D-type ODN do not induce pDC maturation, do not activate B cells directly and have reduced pro-inflammatory effects (6,8). Previous studies demonstrated that administration of ODN type D, but not K or C ODN, improves the clinical outcome in health and immunocompromised non-human primates challenged with *Leishmania major* [(9,10) and D. Verthelyi, unpublished data].

Unlike K and C-type ODN, which have several CpG motifs and phosphorothioate backbones to increase resistance to nucleases, CpG ODN type D are characterized by having a core sequence with a single palindromic purine-pyrimidine-CpG-purine-pyrimidine motif flanked on both sides by 3–5

*To whom correspondence should be addressed at 8800 Rockville Pike, Building 29A, Rm 3B19, Bethesda, MD 20892, USA. Tel: +1 301 827 1702; Fax: +1 301 480 3256; Email: daniela.verthelyi@fda.hhs.gov

The authors wish it to be known that, in their opinion, the first two authors should be regarded as joint First Authors

self-complementary bases on a phosphorodiester backbone. Such a structure renders the sequence flexible allowing for the formation of a stem–loop conformation and/or forming dimers with other D-type ODN molecules (6). In addition, D-type ODN have a 3′ end poly(G) motif (6), which is known to self-associate via Hoogsteen base-pairing to form parallel quadruplex structures called G-tetrads (11,12). CpG ODN type A have a similar general structure, but have poly(G) tracts on both the 3′ and 5′ ends and therefore can form parallel and anti-parallel quadruplex structures (12,13). Recent studies show that the formation of multimers is necessary for D-type ODN to localize to early transferring receptor positive endosomes to signal through TLR-9 and induce IFNα, and that monomeric sequences behave as competitive antagonists (8,13,14). Indeed, disruption of the poly(G) motif by removing them or replacing one or more guanines with adenines or 7-deazaguanosines to impede tetrad formation abrogates the IFNα-inducing activity (6,13,14). However, the poly(G) motif mediated formation of tetrads poses formidable challenges for the synthesis, purification, and characterization of CpG ODN type D, often leading to significant variations between lots and hindering the clinical development of these ODN (12,13,15). To address this issue, we have developed a pro-drug form of CpG ODN type D (Pro-D ODN) in which the backbone of the poly(G) track is functionalized with 2-(*N*-formyl-*N*-methyl)aminoethyl (*fma*) groups. The incorporation of these groups into ODN is achieved during solid-phase synthesis via phosphoramidites **1a–d** [Figure 1, (16,17)]. In this study we assess the structural and immunostimulatory characteristics of pro-D ODN and demonstrate that they have reduced G-tetrad formation and multimerization in solution but retain their *in vitro* and *in vivo* immunomodulatory activity.

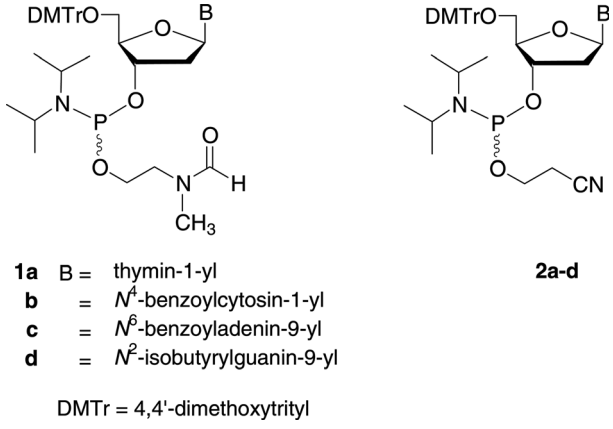

Figure 1. Deoxyribonucleoside phosphoramidites used in the solid-phase synthesis of the oligodeoxynucleotides listed in Table 1.

MATERIALS AND METHODS

Oligodeoxynucleotides

ODN D35, D144, D35 no-pal, DTP9, DTP10, K3, and K2007, were obtained from the FDA core facility. Solid-phase synthesis of pro-D35 and pro-D144 ODN was performed on a scale of 1 μmol using a succinyl long chain alkylamine controlled-pore glass (Succ-LCAA-CpG, 500 Å) support functionalized with N^2-isobutyryl-5′-*O*-DMTr-2′-deoxyguanosine as the leader nucleoside. The syntheses were carried out using a DNA/RNA synthesizer and phosphoramidites **1d** and/or **2a–d** (Figure 1, Table 1) as 0.1 M solutions in dry MeCN. The reaction time for each phosphoramidite coupling step was 180 s. The dedimethoxytritylation step of each chain-elongation cycle was carried out over a period of 60 s. A solution of 0.05 M 3*H*-1,2-benzodithiol-3-one 1,1-dioxide in MeCN was employed as an oxidant during the first two chain-elongation cycles. Each of these sulfuration steps was performed before the capping reaction step, and the reaction time for these steps was 120 and 60 s, respectively. By the third chain-elongation cycle, the sulfurizing reagent was replaced with the commercial oxidizing solution (0.02 M iodine in tetrahydrofuran/pyridine/water) and the capping step was carried out before oxidation over a period of 60 s. By the 18 chain-elongation cycle, the oxidant was replaced with the sulfurizing reagent; the oxidant line was cleaned thoroughly until it was iodine-free. Upon completion of the DNA chain assembly, the 5′-*O*-DMTr group was left intact to facilitate purification of the ODN via reversed-phase high-performance liquid chromatography (RP-HPLC) in both 'trityl-on' and 'trityl-off' modes.

Solid-phase synthesis of ODN *fma*-D35 (Table 1) was prepared under conditions identical to those described above for the preparation of pro-D35 and pro-D144 ODN with the exception of using phosphoramidites **1a–d** (18) exclusively.

Deprotection and purification of pro-D35, pro-D144 and *fma*-D35 ODN was carried out identically as described earlier

Table 1. Synthetic ODN sequences used in this study

ODN	Description	DNA sequence
D35	CpG ODN type D (positive control)	$G^SG^STGCATCGATGCAGGGG^SG^SG$
D144	ODN type D (GpC control)	$G^SG^STGCATGGATGCAGGGG^SG^SG$
Pro-D35	CpG ODN type D [*fma*-protected 3′ poly(G)]	$G^SG^STGCATCGATGCAG*G*G*G*G*^SG$
Pro-D144	ODN type D [*fma*-protected 3′poly(G)]	$G^SG^STGCATGTATGCAG*G*G*G*SG*^SG$
fma-D35	*fma*-protected CpG ODN type D	$G*^SG*^ST*G*C*A*T*C*G*A*T*G*C*A*G*G*G*G*^SG*^SG$
DTP9	CpG ODN type D [no 3′ poly(G)]	$G^SG^STGCATCGATGCATGTG^ST^SG$
DTP10	CpG ODN type D [no 3′ poly(G) and no palindrome]	$G^SG^STGCATCGATATATGTG^ST^SG$
D35 no-pal	CpG ODN type D (no palindrome)	$G^SG^STGCATCGATATAGGGG^SG^SG$
K2007	CpG ODN type K	$T^SC^SG^ST^SC^SG^ST^ST^SG^ST^SC^SG^ST^ST^ST^ST^SG^ST^SC^SG^ST^ST$
K3	CpG ODN type K	$A^ST^SC^SG^SA^SC^ST^SC^ST^SC^SG^SA^SG^SC^SG^ST^ST^SC^ST^SC$

'^{S}' stands for an internucleotidic phosphorothioate diester linkage; '*' corresponds to an internucleotidic 2-(*N*-formyl-*N*-methyl)aminoethyl phosphate triester linkage; '$*^S$' identifies an internucleotidic 2-(*N*-formyl-*N*-methyl)aminoethyl thiophosphate triester linkage.

Table 2. Molecular weight determination of oligodeoxynucleotides by MALDI-TOF mass spectrometry

ODN	Molecular formula	Calcd MW $(M-H)^-$	Exp. MW $(M-H)^-$	Exp. mass error[a] (%)	Exp. MW[b] $(M-H)^-$
D35	$C_{197}H_{224}N_{85}O_{114}P_{19}S_4$	6320	6322	+0.03	6319
Pro-D35	$C_{217}H_{278}N_{90}O_{119}P_{19}S_4$	6764	6763	−0.01	6759
Pro-D144	$C_{218}H_{265}N_{89}O_{120}P_{19}S_4$	6769	6772	+0.04	ND
DTP9	$C_{197}H_{227}N_{76}O_{117}P_{19}S_4$	6248	6244	−0.06	ND
DTP10	$C_{198}H_{229}N_{75}O_{117}P_{19}S_4$	6248	6247	−0.02	ND
D35 no-pal	$C_{199}H_{226}N_{83}O_{115}P_{19}S_4$	6337	6342	+0.08	ND
K2007	$C_{216}H_{255}N_{66}O_{121}P_{21}S_{21}$	7036	7037	+0.01	7031
K3	$C_{193}H_{227}N_{68}O_{102}P_{19}S_{19}$	6329	6327	−0.03	ND

Identity of each ODN was confirmed on the basis of the concordance between its theoretical MW and its MW determined experimentally. ND, not determined.
[a]Experimental mass error is determined according to the following formula: (Exp. MW − Calcd MW)100/Calcd MW.
[b]MW was determined after four freeze/thaw cycles.

(16). The purity of the ODN was assessed by RP-HPLC using an analytical 5 μm Supelcosil LC-18S column under conditions described elsewhere (16).

Oligodeoxynucleotide characterization

ODN were characterized by MALDI-TOF mass spectrometry. Analyses were performed on an instrument operating in delayed extraction reflector mode, using 3-hydroxypicolinic acid [50 mg/ml in MeCN/H_2O (1:1 v/v)] as a matrix and ammonium citrate (50 mg/ml in H_2O) as a cation exchanger. Results are shown in Table 2.

Size exclusion (SEC)-HPLC was performed using a 5 μm TSK-Gel G3000SW_{XL} column (7.8 mm × 30 cm, TOSOH Bioscience) according to the following conditions: 50 μl of an ODN solution (50 μM) in 30 mM sodium chloride was injected into the column. A buffer composed of 10 mM sodium phosphate (pH 6.9) and 300 mM sodium chloride was then pumped, isocratically, through the column at a flow rate of 1 ml/min, over a period of 40 min. Peak heights were normalized to the highest peak, which was set to one arbitrary unit.

PAGE under non-denaturing conditions and circular dichroism (CD) spectroscopy were employed to analyze the secondary/tertiary structure of pro-D35, D35, D35 no-pal, DTP9, DTP10 and K3 ODN. Each lyophilized ODN (0.3–1 OD_{260}) was dissolved in distilled water (10 μl) to which 2 μl of loading buffer (40% sucrose and 0.25% bromophenol blue) was added. The samples were loaded on a native gel (20% polyacrylamide and 1× TBE, pH 8.3) and were electrophoresed at 250 V until the bromophenol blue dye had traveled 20 cm at ~25°C. The gel was then stained using stains-all and processed as described elsewhere (16).

CD analyses were performed under the following conditions: (i) each lyophilized ODN was dissolved in 10 mM Tris, pH 8.5, to a final concentration of 50 μM; (ii) prior to recording the CD spectrum, 50 μl of each ODN solution was diluted further in 10 mM Tris, pH 7.5 (300 μl), or in a solution (300 μl) of 10 mM Tris, pH 7.5, and 100 mM KCl; (iii) CD spectra were recorded in increments of 0.5 nm between 230 and 320 nm, with a 5 s integration time; (iv) for each ODN CD spectrum, a baseline blank was recorded under identical conditions and subtracted from the original CD spectrum using the KaleidaGraph software; and (v) all measurements were performed at 37°C in a cuvette having a 2 mm path length.

All ODN had <0.01 EU/ml as assessed by the Limulus amebocyte lysate assay (Cambrex, Walkersville, MD).

Isolation of cells and cell culture

Elutriated monocytes or human peripheral blood mononuclear cells (PBMC) were provided by the Blood Bank of the National Institutes of Health, Bethesda, MD and separated by density gradient centrifugation over Ficoll–Hypaque as described elsewhere (6). Rhesus macaque PBMC were isolated and processed in the same manner. Cells were cultured at a density of 2×10^6 cells/ml, at 37°C in RPMI-1640 media supplemented with 5% (flow cytometry) or 10% (supernatants) FCS and 100 U penicillin/ml, 100 μg streptomycin/ml, glutamine, non-essential amino acids, HEPES and β-mercaptoethanol as described earlier (9). One micromolar concentration of each ODN was used to stimulate cytokine production, dendritic cell maturation and activation. Cell viability after 72 h was >95% as assessed by trypan blue staining.

Cellular CpG ODN binding and uptake. D35, K3, and pro-D35 ODN were labeled, each with fluorescein isothiocyanate (FITC) as described previously (19). Two million monocytes were incubated with 3 μM CpG ODN-FITC in 1× PBS for 30 min, at 37°C. Cells were washed twice with PBS–1% BSA–0.1% sodium azide and resuspended in 0.5 ml of flow cytometry buffer. Fluorescence was determined using a FACSCalibur flow cytometer (BD Biosciences, San Jose, CA) (total FITC MFI value). Subsequently, surface fluorescence was quenched by adding 0.5 ml of 1:1 trypan blue in PBS over a period of 5 min on ice (intracellular FITC). The percentage of internalized ODN was calculated from the following ratio: (intracellular FITC MFI value/total FITC MFI value) × 100.

ELISA. Cytokine production was assessed as reported earlier (20). Briefly, 96-well microtiter plates (Immunolon 2; Dynex Inc., Chantilly,VA) were coated with anti-cytokine antibody (Ab) and blocked with PBS–5% BSA. Supernatants from PBMC cultures were added, and their cytokine content quantified by the addition of biotin-labeled anti-cytokine Ab followed by phosphatase-conjugated avidin and phosphatase-specific colorimetric substrate. Standard curves were generated using known amounts of recombinant human cytokine. All assays were performed in triplicate.

Flow cytometry. To assess monocyte-derived DC maturation and activation, cell cultures were stimulated with 1 μM ODN for 48 h, then fixed and analyzed by flow cytometry. Staining for cell surface markers was performed using FITC-conjugated anti-CD14, PE-conjugated anti-CD83 and PECy5-conjugated anti-CD86 Abs (BD/Pharmingen, San Diego, CA). Multi-parameter flow cytometry was performed according to standard protocols (5) in a FACSCalibur flow cytometer. Profiles were gated on monocytes and 60 000–250 000 total events were collected. Results were analyzed using the FlowJo software (Tree Star, Inc., OR).

Infection protocol

Rhesus macaques. Healthy 2–3 year old rhesus macaques (*Macaca mulata*, four per group) were obtained from the FDA colony in South Carolina. All studies were IACUC approved and were conducted in an AAALAC accredited facility. Animals were monitored daily. No changes in weight, appetite, demeanor or skin modifications were evident during infection or treatment. Treatments were administered and peripheral blood samples obtained from ketamine-anesthetized animals (10 mg/kg, Ketaject; Phoenix Pharmaceuticals, St Joseph, MD).

Leishmania major. *L.major* clone VI promastigotes (MHOM/IL/80/Friedlin) were grown as described in the literature (21). Macaques were randomly assigned to treatment groups and then challenged intradermally in the forehead with 1×10^6 parasites per site, at three sites 3 cm apart, and treated with 500 μg/kg CpG ODN (subcutaneous in the inter-scapular space) 3 days before and 3 days after challenge, or left untreated. Monkeys inoculated with live metacyclic promastigotes developed a typical self-limited *in situ* lesion characterized by erythema, induration, and ulceration that resolved in 8–12 weeks. Lesion size, which reflects the severity of infection, was measured weekly in a blinded fashion.

ELIspot. The number of PBMC secreting IFNα, IP-10 and IFNγ in response to CpG ODN or soluble *Leishmania* antigen (SLA) was determined by ELIspot as described earlier (21). Briefly, Immunolon 2 96-well plates were coated overnight at 4°C with 1 μg/ml of anti-human IFNα (PBL, Piscataway, NJ), IFNγ (Clone GZ4; Alexis, San Diego, CA) or IP-10 antibodies (R & D systems, Minneapolis, MN) in PBS and then blocked with PBS–5% BSA for 1 h. The plates were overlaid with $0.1–2 \times 10^5$ cells/well in triplicates and incubated at 37°C in a humidified 5% CO_2 in air incubator for 12 h (IFNα) or 24 h (IP-10) with 1 μM of CpG ODN, or 18 h in the presence of 25 μg/ml SLA or 10 μg/ml of ovalbumin. After washing, 1 μg/ml of biotin-conjugated anti-human IFNα (PBL), anti-IP-10 (R & D Systems) or anti-IFNγ antibody (clone 76-B-1; Mabtech, Sweden) were added and plates were incubated for 2 h, washed and subsequently overlaid with alkaline phosphatase-conjugated streptavidin. Spots were visualized by the addition of 5-bromo-4-chloro-3-indolyl phosphate (Sigma, St Louis, MO)in low melt agarose (Sigma).

Statistical analysis

Differences in lesion sizes were tested by repeated-measures ANOVA using the Proc Mixed procedure from the statistical analysis system. One-way ANOVA was used to test differences in cytokine levels and cytokine secreting cells.

RESULTS AND DISCUSSION

Reduced G-tetrad formation of pro-CpG type D in K^+-free media

Pro-D35 was synthesized and purified as described above using phosphoramidite **1d**, so that five internucleotidic linkages of the ODN poly(G) tract were functionalized with *fma* groups. MALDI-TOF MS analysis of purified pro-D35 ODN (Table 2) revealed an experimental molecular weight (MW) within 0.1% of its calculated MW, thereby confirming the ODN's identity.

To assess the presence of ODN multimerization, K, D and pro-D ODN were analyzed by PAGE under non-denaturing conditions. As reported previously for CpG ODN type A (14) several bands were observed for D35 ODN, indicating that poly(G) bearing ODN exist as a mixture of monomeric, dimeric and multimeric structures (Figure 2A). The bands corresponding to the multimerized forms of D35 vanished when the sample was heated for 20 min at 96°C and immediately cooled on ice (data not shown). The self-complementary motif appears to be required for the formation of dimers as D35 no-pal showed bands corresponding to the monomer and high-order multimer, but not dimers. Despite having the same sequence as D35, pro-D35, similar to DTP9 which lacks the poly(G) tract, showed a major band corresponding to the dimeric form and a minor one corresponding to the monomeric form. The dimer band for pro-D35 exhibited a slower electrophoretic mobility and a lighter staining pattern when compared with the dimeric form of the parental D35, thereby reflecting reduction of the charge/mass ratio of pro-D35 ODN. The decreased multimerization of pro-D35 was confirmed by size exclusion HPLC. As shown in Figure 2B, pro-D35 and K ODN eluted as single peaks, whereas D35 showed additional peaks reflecting a mixture of monomeric and multimeric forms.

The 3′ poly(G) motif of D-type ODN is known to contribute to multimerization through formation of G-tetrad structures (13,14). CD studies showed that D35 displays a characteristic parallel-stranded quadruplex spectrum with maximal ellipticity at ~265 nm and a minimal ellipticity ~240 nm (Figure 2C). However, as shown by the CD spectrum of D35 no-pal, tetrad formation did not require the dimerization of the ODN through self-complementary far-flanking regions. This spectrum was different from the CD signature of K3 ODN or DTP9, which do not have poly(G) sequences, and showed a maximum and minimum ellipticity at ~280 nm and ~260 nm, respectively, a pattern associated with monomeric sequences (Figure 2C). When recorded in the presence of 100 mM KCl (a potassium concentration similar to that of an intracellular milieu), the CD profile of either ODN was unchanged. In contrast, pro-D35 showed a CD profile similar to that of DTP9 in the absence of KCl (maximum ellipticity at ~275 nm), but displayed one consistent with G-tetrad formation in the presence of KCl (100 mM) (Figure 2C).

A previous study had shown that *fma* thiophosphate or phosphate protecting groups are thermolytically cleaved off the ODN with a half time of 72 h or 56 h, respectively, at 37°C (16). Our own analysis of the impact of temperature on tetrad formation showed that D35 and K2007 ODN maintained their tertiary (tetrad/no tetrad) structure over time (data

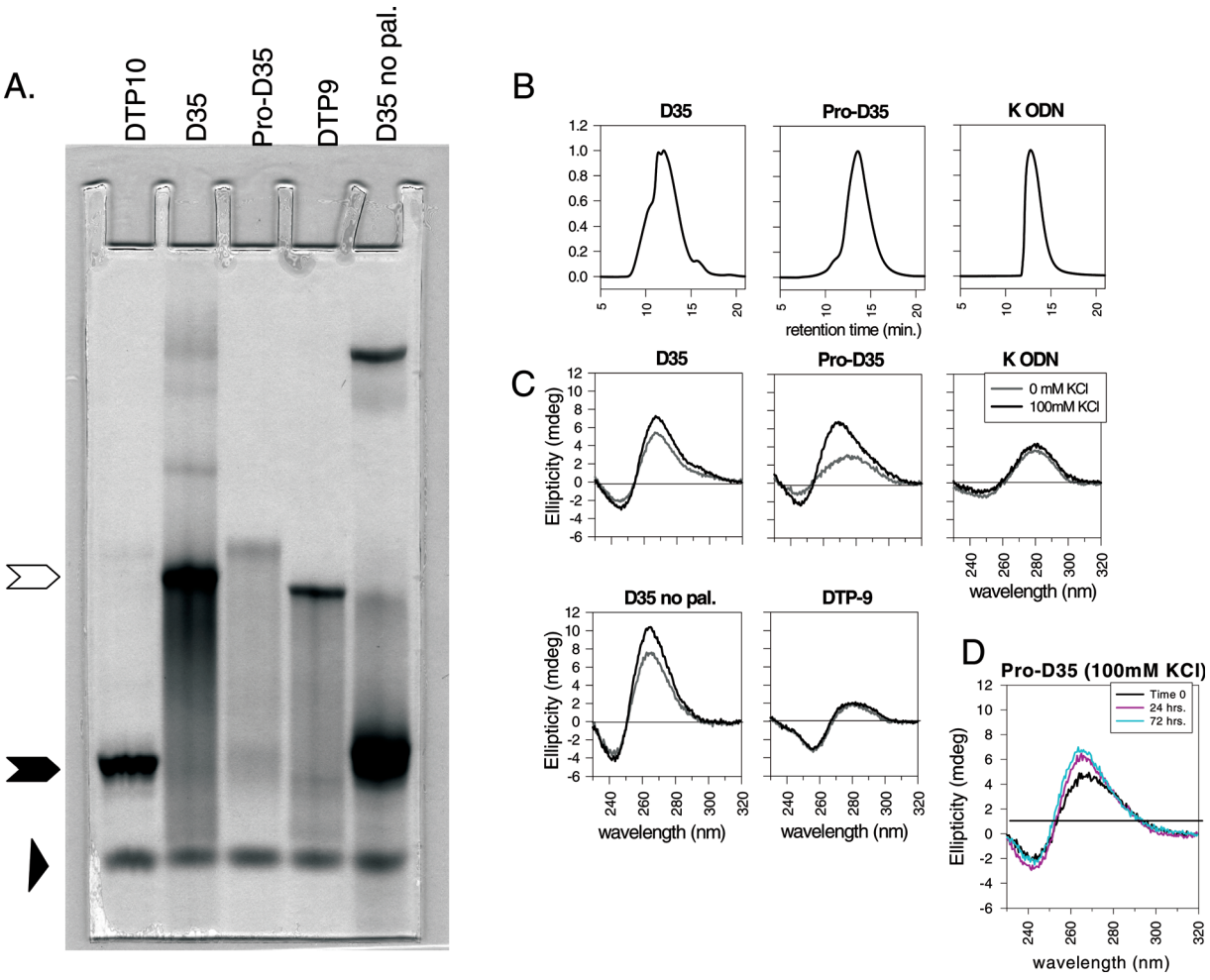

Figure 2. Secondary structure and multimerization: (**A**) ODNs (0.3–1 OD_{260}) were analyzed by gel electrophoresis under non-denaturing conditions (20% polyacrylamide and 1× TBE, pH 8.3) at ~25°C. The gel was electrophoresed at 250 V until the bromophenol blue marker (fastest moving band marked with black triangle) had traveled 20 cm, and was then stained with Stains-all. Electrophoretic mobility of monomeric ODN is indicated by a solid arrow, whereas the open arrow shows the mobility of ODN exhibiting secondary structures and/or self-complementary dimerization. Controls (not shown) included: boiled D 35 and K2007 (Table 1). Note that ODN with 3′ poly(G) tracts (D35, D35 no-pal) have higher order structures that are absent when the poly(G) sequence is deleted (DTP9 and DTP10) or protected with *fma* groups (pro-D35). (**B**) Aggregate formation assessed by size-exclusion HPLC using a TSK-gel column. Solutions of D35, pro-D35 and K3 were prepared in 30 mM NaCl. (**C**) G-tetraplex formation monitored by circular dichroism (CD) spectroscopy in the presence and absence of KCl. The presence of G-tetrad is characterized by a maximal positive ellipticity at ~265 nm and a minimal negative ellipticity near 240 nm (D35 ODN). CD units are in millidegrees. In the absence of G-tetrad (CpG ODN type K), the maximal positive and minimal negative ellipticities are shifted to ~280 nm and ~260 nm, respectively. Note that the CD spectrum of pro-D35 shows the absence of G-tetrad formation in the absence of potassium salt, whereas the signature of G-tetrad formation is detected in the presence of potassium salt. (**D**) Time course showing changes in the CD spectra of pro-D35 over time in the presence of potassium salt (100 mM KCl, 37°C).

not shown). In contrast, the CD spectrum of pro-D35 ODN in the presence of potassium at 37°C (Figure 2D) showed a progressive increase in G-quadruplex signature over a period of 72 h suggesting that with time, the formation of G-tetrads is commensurate with the thermolytic conversion of pro-D35 to D35. Together these data strongly suggest that pro-D ODN do not form G-quadruplex structures in solutions low in potassium salt concentrations but can form G-tetrads inside the cell where the concentrations of potassium are higher. Further, the G-tetrads become more stable with time as the thermolytic moieties are cleaved.

Cellular uptake and immunostimulatory properties of pro-D ODN

CpG ODN interact with TLR-9 within early endosomes; thus cellular uptake must occur prior to signaling (22,23). Although cellular uptake is CpG motif-independent, studies have shown that poly(G) motifs increase ODN internalization and alter their intracellular location (8,19,24,25). It was therefore important to assert whether changing the ODN structure and the polarity of the poly(G) tract would interfere with cellular uptake. Binding and internalization of FITC-labeled ODN was assessed by flow cytometry as previously reported (19). Cellular binding of pro-D35 was 80.6 ± 2.8% that of parental D35, but the change in polarity of the protected poly(G) sequence did not affect ODN internalization (Figure 3). Indeed, even when all the internucleotidic phosphate/thiophosphate linkages of D35 were protected with *fma* groups (*fma*-D35 ODN), there was no significant reduction in ODN internalization suggesting that cellular uptake of CpG ODN is independent of its polarity and of G-tetrad formation. Furthermore, PBMC stimulated with

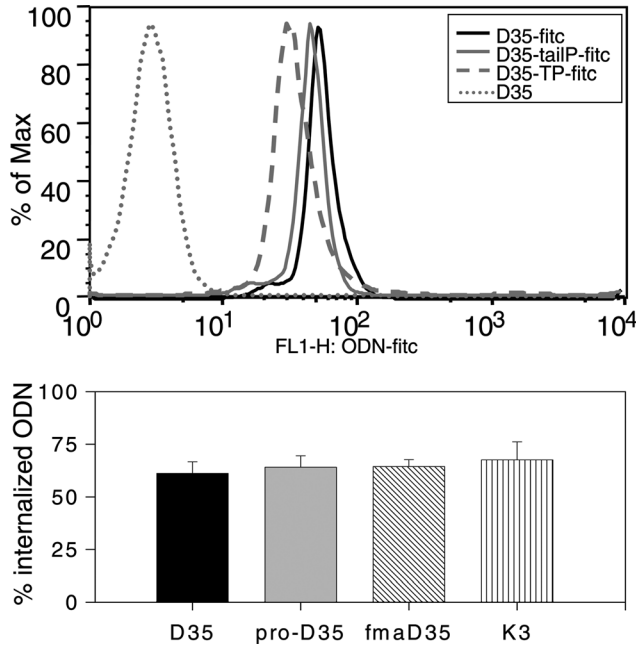

Figure 3. Cellular binding and uptake of pro-ODN. Binding and uptake by elutriated monocytes were measured by flow cytometry using FITC-labeled ODN (3 μM, 30 min at 37°C). (**A**) Shows similar total fluorescence (binding and uptake) for D35 and pro-D35 (Data are representative of five independent experiments). (**B**) Percent internalized ODN relative to total fluorescence. Fluorescence of surface-bound ODN was quenched using trypan blue staining (1:4 dilution, 10 min on ice) and calculated as follows: (MFI of internalized fluorescence/MFI of total fluorescence) × 100.

pro-D35 *in vitro* for 72 h induced secretion of IFNα, IL-6, IP-10 and IFNγ to levels that were similar to those achieved with D35 (Figure 4A). In contrast, *fma*-D35, despite uptake, did not induce an increase in cytokine/chemokine levels (data not shown). Finally, pro-D35 was as effective as D35 in inducing monocytes to mature into myeloid DC after 48 h in culture, as inferred by expression of CD83, CD86, CD14, MHC II and CD40 (Figure 4B and data not shown), whereas *fma*-D35 failed to drive DC maturation (Figure 4B).

Recent studies suggest that the differential effect of B (also called K) and D ODN is linked to the type of endosome they localize to and propose that ODN that form multimers are retained in the early and recycling endosomes while monomeric ODN are rapidly transferred to LAMP-1-positive late endosomes and lysosomes (8,14). Other studies suggest it is not size or the formation of multimers, but instead their ability to bind cells surface scavenger receptors such as CXCL16 what determines the type of signaling cascade that will ensue stimulation (25). Regardless of the mechanism by which D ODN trigger TLR-9 in the early endosomes, the use of thermolytic *fma* groups to reduce tetrad formation by poly(G) bearing ODN did not significantly impact on the ODN's uptake or immunomodulatory activity. This suggests that the addition of formyl groups to the poly(G) strand does not alter the intracellular localization or the signaling cascade initiated by pro-D35. In contrast, placement of protective groups on the CpG motif prevents its immunomodulatory activity suggesting that they would interfere with the activation of TLR-9.

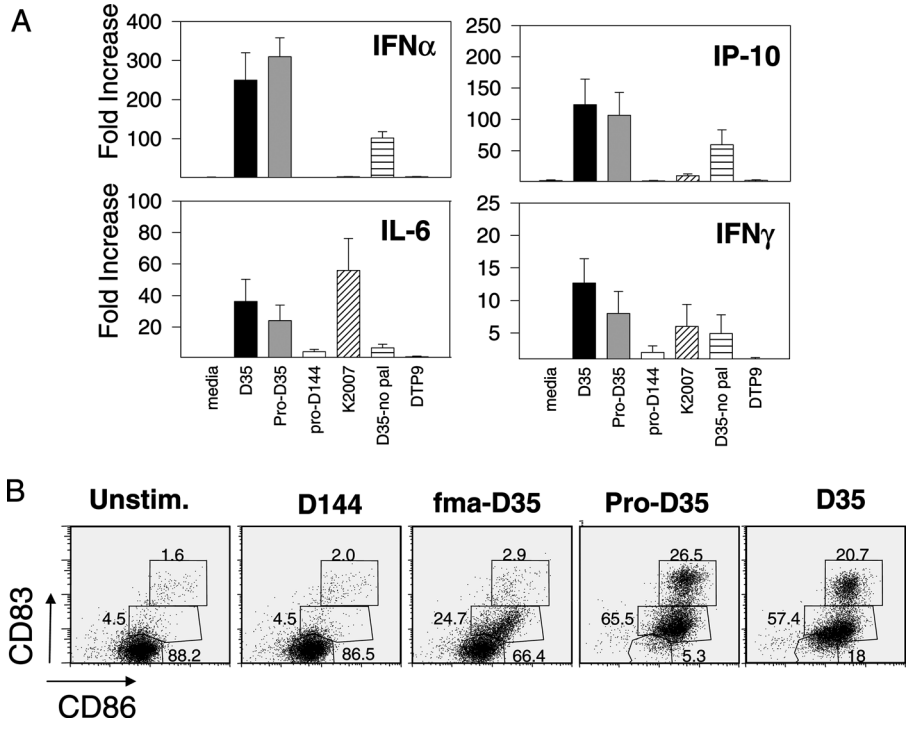

Figure 4. Immunomodulatory effect of pro-D35 *in vitro*: (**A**) Response of human PBMC to pro-D35. IFNα, IFNγ, IL-6 and IP-10 levels were quantified by ELISA in 72 h supernatants PBMC from eight healthy donors. Note that pro-D35 and D35 induced similar cytokine levels. (**B**) CpG ODN type D mediated differentiation of monocytes into mature DC. Elutriated monocytes were incubated with 1 μM ODN for 48 h. Cells were fixed and stained for expression of CD83 and CD86. (Results are representative of five independent experiments.)

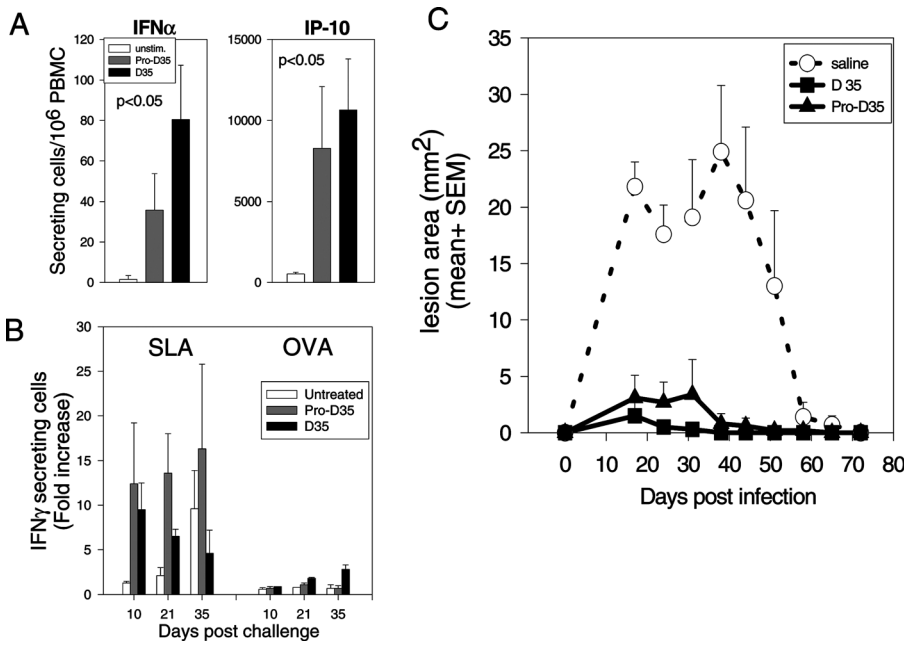

Figure 5. Immunomodulatory effect of pro-D35 in rhesus macaques. (**A**) Response of PBMC from healthy rhesus macaques to CpG ODN stimulation *in vitro*. Three days after CpG ODN treatment, the number of IFNα and IP-10 secreting cells was assessed by ELIspot after 12 and 24 h of *in vitro* stimulation, respectively. Statistical significance was determined by one-way ANOVA. (B/C) Rhesus macaques ($n = 4$/group) were challenged with 10^6 *L.major* metacyclic promastigotes (intradermally) and treated with CpG ODN (supracutaneously; 0.5 mg/kg) 3 days before and after challenge. Saline-treated macaques served as controls. (**B**) IFNγ-secreting PBMC in macaques challenged with *L.major* and re-stimulated *in vitro* with soluble *Leishmania* antigen (SLA) or unrelated protein (ovalbumin) were determined by ELIspot at specified time points. (**C**) Development of cutaneous lesions in response to *L.major* infection and CpG ODN treatment. Figure shows average size of the lesion calculated as: $[\text{mean diameter}/2]^2 \times \pi$. Note that the lesion size from macaques treated with D35 or pro-D35 ODN peaked earlier and were smaller ($P < 0.05$) than those in untreated macaques.

Immunoprotective effect of pro-D ODN

Asian rhesus macaques (*M.mulata*) have been used previously to assess the activity of CpG ODN in primates, as their immune cells respond to the same CpG ODN sequences as human PBMC (26,27). Pro-D35 and D35 induced a significant increase in the number of cells secreting IFNα and IP-10 upon stimulation *in vitro* (Figure 5A). The immunoprotective activity of pro-D35 was then assessed *in vivo* in rhesus macaques challenged intradermally with 3×10^6 live *L.major* metacyclic promastigotes. This animal model of cutaneous leishmaniasis has been used previously to demonstrate the immunoprotective effect of CpG ODNs type D (10,21). Specifically, animals treated with D-type ODN, but not with CpG ODN type K or type C, developed significantly smaller lesions than untreated animals (D. Verthelyi, unpublished data). Twelve macaques (four/group) were treated, subcutaneously, in the inter-scapular space with D35 or pro-D35 ODN (0.5 mg/kg) 3 days before and after challenge or left untreated. These macaques developed a self-limited nodular skin lesion at the site of inoculation similar to those observed in human cutaneous leishmaniasis (28). Animals treated with D35 or with pro-D35 ODN around infection time developed significantly smaller lesion size as compared with untreated ones (Figure 5B). The reduction in lesion size was associated with a significant increase in the number of antigen-specific cells secreting IFNγ early in disease progression ($P < 0.05$; Figure 5C). These data demonstrate that pro-D ODN are active and effective *in vivo*. Importantly, no losses of weight, lymphadenopaties, or other adverse events were observed during the study suggesting that these ODN do not induce overt adverse effects at therapeutic doses.

This report is the first to demonstrate the biological activity of a pro-drug form of CpG ODN type D developed by incorporating *fma* groups into the backbone of the 3′ poly(G) end (pro-D35 ODN). These protecting groups provided a transitory reduction of G-tetrad formation in potassium-free solutions, while allowing tetrad formation when potassium salt concentrations mimicked those of an intracellular environment (~100 mM). This modification did not significantly affect cellular uptake or biological activity, as shown by increased cytokine production and DC maturation, which were comparable to that effected by the parental D35 ODN. Finally, the clinical potential of pro-D35 ODN was demonstrated through the significant reduction of lesion severity in *Leishmania*-infected rhesus macaques. The current findings may have implications in other therapeutic oligonucleotides venues, such as in anti-sense and siRNA applications, especially when the administration of these ODNs as prodrugs may confer a therapeutic advantage.

ACKNOWLEDGEMENTS

The authors thank Dr Joao Pedras-Vasconcelos and Dr David Davies for reviewing the manuscript. The L. major parasites were a kind gift of Dr David Sacks, NIAID. In addition, we thank Dr Phil Snoy, Dr Brianna Skinner-Harris, Ray Olsen and the Animal Care Facility staff for their care of the non-human primates included in this study. C.A. is a fellow at the

Postgraduate Research Participation Program at the Center for Drug Evaluation and Research administered by the Oak Ridge Institute for Science and Education through an interagency agreement between the US Department of Energy and the US Food and Drug Administration. The assertions herein are the private ones of the authors and are not to be construed as official or as reflecting the views of the Food and Drug Administration at large. Funding to pay the Open Access publication charges was provided by the Office of Pharmaceutical Sciences, Office of Biotechnology Products, CDER, FDA.

Conflict of interest statement. Serge Beaucage, Andrzej Grajkowski and Daniela Verthelyi are named as inventors on a patent application related to these oligonucleotides. There are no other conflicts to declare.

REFERENCES

1. Krieg,A.M. (2006) Therapeutic potential of Toll-like receptor 9 activation. *Nature Rev. Drug Discov.*, **5**, 471–484.
2. Klinman,D.M. (2004) Immunotherapeutic uses of CpG oligodeoxynucleotides. *Nature Rev. Immunol.*, **4**, 249–258.
3. Bauer,S., Kirschning,C.J., Hacker,H., Redecke,V., Hausmann,S., Akira,S., Wagner,H. and Lipford,G.B. (2001) Human TLR9 confers responsiveness to bacterial DNA via species-specific CpG motif recognition. *Proc. Natl Acad. Sci. USA*, **98**, 9237–9242.
4. Verthelyi,D. and Zeuner,R.A. (2003) Differential signaling by CpG DNA in DCs and B cells: not just TLR9. *Trends Immunol.*, **10**, 519–522.
5. Gursel,M., Verthelyi,D. and Klinman,D.M. (2002) CpG oligodeoxynucleotides induce human monocytes to mature into functional dendritic cells. *Eur. J. Immunol.*, **32**, 2617–2622.
6. Verthelyi,D., Ishii,K.J., Gursel,M., Takeshita,F. and Klinman,D.M. (2001) Human peripheral blood cells differentially recognize and respond to two distinct CpG motifs. *J. Immunol.*, **166**, 2372–2377.
7. Krug,A., Rothenfusser,S., Hornung,V., Jahrsdorfer,B., Blackwell,S., Ballas,Z.K., Endres,S., Krieg,A.M. and Hartmann,G. (2001) Identification of CpG oligonucleotide sequences with high induction of IFNa/b in plasmacytoid dendritic cells. *Eur. J. Immunol.*, **31**, 2154–2163.
8. Guiducci,C., Ott,G., Chan,J.H., Damon,E., Calacsan,C., Matray,T., Lee,K.D., Coffman,R.L. and Barrat,F.J. (2006) Properties regulating the nature of the plasmacytoid dendritic cell response to Toll-like receptor 9 activation. *J. Exp. Med.*, **203**, 1999–2008.
9. Verthelyi,D., Kenney,R.T., Seder,R.A., Gam,A.A., Friedag,B. and Klinman,D.M. (2002) CpG oligodeoxynucleotides as vaccine adjuvants in primates. *J. Immunol.*, **168**, 1659–1663.
10. Verthelyi,D., Gursel,M., Kenney,R.T., Lifson,J.D., Shuying,L., Mican,J. and Klinman,D.M. (2003) CpG Oligodeoxynucleotides protect normal and SIV infected macaques from Leishmania infection. *J. Immunol.*, **170**, 4717–4723.
11. Panyutin,I.G., Kovalsky,O.I., Budowsky,E.I., Dickerson,R.E., Rikhirev,M.E. and Lipanov,A.A. (1990) G-DNA: A twice-folded DNA structure adopted by single-stranded oligo(dG) and its implications for telomeres. *Proc. Natl Acad. Sci. USA*, **87**, 867–870.
12. Costa,L.T., Kerkmann,M., Hartmann,G., Endres,S., Bisch,P.M., Heckl,W.M. and Thalhammer,S. (2004) Structural studies of oligonucleotides containing G-quadruplex motifs using AFM. *Biochem. Biophys. Res. Commun.*, **313**, 1065–1072.
13. Wu,C.C.N., Lee,J., Raz,E., Corr,M. and Carson,D. (2004) Necessity of oligonucleotide aggregation for Toll-like receptor 9 activation. *J. Biol. Chem.*, **279**, 33071–33078.
14. Kerkmann,M., Costa,L.T., Richter,C., Rothenfusser,S., Battiany,J., Hornung,V., Johnson,J., Englert,S., Ketterer,T., Heckl,W. *et al.* (2005) Spontaneous formation of nucleic acid-based nanoparticles is responsible for high interferon-{alpha} induction by cpg-a in plasmacytoid dendritic cells. *J. Biol. Chem.*, **280**, 8086–8093.
15. Marshall,J.D., Fearon,K., Abbate,C., Subramanian,S., Yee,P., Gregorio,J., Coffman,R.L. and Van Nest,G. (2003) Identification of a novel CpG DNA class and motif that optimally stimulate B cell and plasmacytoid dendritic cell functions. *J. Leukoc. Biol.*, **73**, 781–792.
16. Grajkowski,A., Pedras-Vasconcelos,J., Wang,V., Ausin,C., Hess,S., Verthelyi,D. and Beaucage,S.L. (2005) Thermolytic CpG-containing DNA oligonucleotides as potential immunotherapeutic prodrugs. *Nucleic Acids Res.*, **33**, 3550–3560.
17. Grajkowski,A., Cieslak,J., Chmielewski,M.K., Marchan,V., Phillips,L.R., Wilk,A. and Beaucage,S.L. (2003) Conceptual 'heat-driven' approach to the synthesis of DNA oligonucleotides on microarrays. *Ann. NY Acad. Sci.*, **1002**, 1–11.
18. Grajkowski,A., Wilk,A., Chmielewski,M.K., Phillips,L.R. and Beaucage,S.L. (2001) The 2-(*N*-formyl-*N*-methyl)aminoethyl group as a potential phosphate/thiophosphate protecting group in solid-phase oligodeoxyribonucleotide synthesis. *Org. Lett.*, **3**, 1287–1290.
19. Gursel,M., Verthelyi,D., Gursel,I., Ishii,K.J. and Klinman,D.M. (2002) Differential and competitive activation of human immune cells by distinct classes of CpG oligodeoxynucleotide. *J. Leukoc. Biol.*, **71**, 813–820.
20. Zeuner,R.A., Klinman,D.M., Illei,G., Yarboro,C., Ishii,K.J., Gursel,M. and Verthelyi,D. (2003) Response of peripheral blood mononuclear cells from lupus patients to stimulation by CpG oligodeoxynucleotides. *Rheumatology (Oxford)*, **42**, 563–569.
21. Flynn,B., Wang,V., Sacks,D.L., Seder,R.A. and Verthelyi,D. (2005) Prevention and treatment of cutaneous Leishmaniasis in primates by using synthetic type D/A oligodeoxynucleotides expressing CpG motifs. *Infect. Immun.*, **73**, 4948–4954.
22. Ahmad-Nejad,P., Hacker,H., Rutz,M., Bauer,S., Vabulas,R.M. and Wagner,H. (2002) Bacterial CpG-DNA and lipopolysaccharides activate Toll-like receptors at distinct cellular compartments. *Eur. J. Immunol.*, **32**, 1958–1968.
23. Latz Schoenmeyer,A., Visintin,A., Fitzgerald,K.A., Monks,B.G., Knetter,C.F., Lien,E., Nilsen,N.J., Espevik,T. and Golenbock,D.T. (2004) TLR9 signals after translocating from the ER to CpG DNA in the lysosome. *Nature Immunol.*, **5**, 190–198.
24. Bartz,H., Mendoza,Y., Gebker,M., Fischborn,T., Heeg,K. and Dalpke,A. (2004) Poly-guanosine strings improve cellular uptake and stimulatory activity of phosphodiester CpG oligonucleotides in human leukocytes. *Vaccine*, **23**, 148–155.
25. Gursel,M., Gursel,I., Mostowski,H.S. and Klinman,D.M. (2006) CXCL16 influences the nature and specificity of CpG-induced immune activation. *J. Immunol.*, **177**, 1575–1580.
26. Hartmann,G., Weeratna,R.D., Ballas,Z.K., Payette,P., Blackwell,S., Suparto,I., Rasmussen,W.L., Waldshmidt,M., Sajuthi,D., Purcell,R.H. *et al.* (2000) Delineation of a CpG phosphorothioate oligodeoxinucleotide for activating primate immune responses *in vitro* and *in vivo*. *J. Immunol.*, **164**, 1617–1624.
27. Verthelyi,D. and Klinman,D.M. (2003) Immunoregulatory activity of CpG oligonucleotides in humans and nonhuman primates. *Clin. Immunol.*, **109**, 64–71.
28. Amaral,V.F., Ransatto,V.A.O., Conceicao-Solva,F., Molinaro,E., Ferreira,V., Coutinho,S.G., McMahon-Pratt,D. and Grimaldi,G. (1996) *Leishmania amazonensis*: The asian rhesus macaques (*Macaca mulata*) as an experimental model for the study of cutaneous leishmaniasis. *Exp. Parasitol.*, **82**, 34–44.